


10
Three-dimensional tissue model in direct contact with an on-chip vascular bed enabled by removable membranes†

Cite this: DOI: 10.1039/d1lc00751c

 15
 Yoshikazu Kameda, ^a Surachada Chuaychob,^a Miwa Tanaka,^b Yang Liu, ^a Ryu Okada,^a Kazuya Fujimoto,^a Takuro Nakamura^b and Ryuji Yokokawa ^{*a}

 15
 Q1

 20
 25
 Three-dimensional (3D) tissue culture is a powerful tool for understanding physiological events. However, 3D tissues still have limitations in their size, culture period, and maturity, which are caused by the lack of nutrients and oxygen supply through the vasculature. Here, we propose a new method for culturing a 3D tissue—a spheroid—directly on an ‘on-chip vascular bed’. The method can be applied to any 3D tissue because the vascular bed is preformed, so that angiogenic factors from the tissue are not necessary to induce vasculature. The essential component of the assay system is the removable membrane that initially separates the 3D tissue culture well and the microchannel in which a uniform vascular bed is formed, and then allows the tissue to be settled directly onto the vascular bed following its removal. This *in vitro* system offers a new technique for evaluating the effects of vasculature on 3D tissues.

 Received 24th August 2021,
Accepted 1st January 2022

DOI: 10.1039/d1lc00751c

rsc.li/loc

Introduction

 30
 35
 40
 45
 Three-dimensional (3D) tissues are powerful tools for exploring physiological events in detail and are expected to be widely used for drug screening and disease modelling assays. For example, studies have reported the use of multicellular spheroids as tumour models¹ and the *in vitro* culture of embryonic organs as a 3D tissue model for investigating developmental events.² In addition, organoids—3D mini-organs derived from human pluripotent stem cells—have been generated for the liver,³ brain,^{4,5} and kidney.^{6–9} However, current static culture methods limit the size and developmental maturity of 3D tissues that can be achieved. Although external shear stress has been shown to enhance the vascularisation of 3D tissues,¹⁰ only animal transplantation has been reported to enable the perfusable vascularisation of 3D tissues prepared *in vitro* and facilitate their maturation.^{11–13} Therefore, it is important to consider the perfusability of 3D tissues in terms of blood flow as a factor to improve their maturation *in vitro*.

Microfluidic devices are widely used to mimic the perfusability of the cell culture environment as they allow cell position, growth factor gradients, and flow rates to be

 30
 35
 40
 45
 controlled.¹⁴ Previously, Kim *et al.* reported the construction of a perfusable vascular network in a microfluidic device based on the self-organising functions of human umbilical vein endothelial cells (HUVECs).¹⁵ In addition, 3D tissues such as lung fibroblast,^{16–18} neuron,¹⁹ and tumour²⁰ spheroids have been co-cultured with a vascular network. Typically, microfluidic devices contain multiple parallel channels that are separated by micro-posts: 3D tissues are introduced into one of the channels with a hydrogel. Vascular endothelial cells (ECs) are either simultaneously injected into the same channel as the tissue or injected into tissue-adjacent channels. Subsequently, vasculogenic and/or angiogenic sprouts invade the hydrogel and construct a vascular network that is perfusable and sensitive to shear stress¹⁵ and cellular interactions,^{21–23} thereby inducing dynamic remodelling of the network. Hence, on-chip vascular models based on self-organising functions, such as vasculogenesis and angiogenesis, are advantageous for 3D tissue culture but are not readily applicable.

 There are several reasons why such on-chip vascular models are not commonly used for 3D tissue culture. Firstly, 3D tissues are required to provide angiogenic factors in most self-organising models, wherein ECs and a 3D tissue are simultaneously introduced into a device, and growth factors secreted by the tissue induce vascular formation.^{16–20} Therefore, 3D tissues without the ability to induce neovascularisation cannot produce a co-culture model with a vascular network using current self-organising models. The second major issue involves the interaction between vascular networks and 3D tissues, which are closely localised *in vivo*
^a Department of Micro Engineering, Kyoto University, Kyoto Daigaku-Katsura, Nishikyo-ku, Kyoto 615-8540, Japan. E-mail: yokokawa.ryuji.8c@kyoto-u.ac.jp

^b Division of Carcinogenesis, The Cancer Institute, Japanese Foundation for Cancer Research, Tokyo, Japan

† Electronic supplementary information (ESI) available. See DOI: 10.1039/d1lc00751c

in contact with the extracellular matrix (ECM), which mediates a uniform gradient of growth factors, nutrients, and oxygen to support tissue growth. However, *in vitro* vascular networks must be separated from the 3D tissue culture chamber by a polydimethylsiloxane (PDMS) porous membrane since HUVEC vasculature self-organisation requires the ECM to be confined in a microfluidic channel.²⁴ Consequently, biochemical interactions between the tissue and vascular network are limited by the pores of the membrane, unlike the environment *in vivo*.

To overcome these limitations, we created a microfluidic device for co-culturing a vascular network and 3D tissue, which we termed an 'on-chip vascular bed'. The device is first formed using growth factors secreted by human lung fibroblasts (hLFs), which are widely used to form perfusable vascular networks.¹⁵ Once the alginate or polyester membrane separating the vascular bed and 3D tissue culture well has been removed, the 3D tissue is cultured in direct contact with the bed, without any boundary material. In this study, we used a 3D tissue model spheroid composed of HUVECs and hLFs, which has previously been shown to induce angiogenic behaviour in microfluidic devices.^{16,17,20} The spheroid was cultured on the vascular bed under static conditions, and the vascular connection between them was observed. We also demonstrated the applicability of our system using a spheroid containing cells from alveolar soft part sarcoma (ASPS), a rare, slow-growing, and highly metastatic sarcoma that affects adolescents and young adults.²⁵ Together, the findings of this study demonstrate

that this *in vitro* culture system provides a novel method for evaluating the effects of vasculature on 3D tissues.

Materials and methods

Design of the microfluidic device

The microfluidic device included a vascular bed and a spheroid, as illustrated in Fig. 1a, and consisted of four parts: a top layer with gel injection ports, medium inlets, and a spheroid culture well; a bottom layer with an open top and five parallel channels separated by micro-posts; a separation membrane; and a glass coverslip (Fig. 1b).²⁶ Initially, the spheroid culture well and channels were separated by a membrane to contain the solution within the bottom channels. Two materials were used for the membrane: alginate and polyester, with devices containing each type, designated AM and PM, respectively. The alginate membrane was dissolved using a chelating agent (*e.g.*, ethylenediaminetetraacetic acid [EDTA]),²⁷ whereas the polyester membrane was easily removed with tweezers. The detailed configuration of the bottom layer is shown in Fig. S1.† HUVECs were cultured in channel 3, and hLFs were cultured in channels 1 and 5. The growth factors secreted by hLFs promoted vascular bed formation.

Fabrication of the microfluidic device

The bottom layer was fabricated using conventional soft lithography: SU-8 2100 (MicroChem, Westborough, MA, USA) was photolithographically patterned onto a silicon wafer with

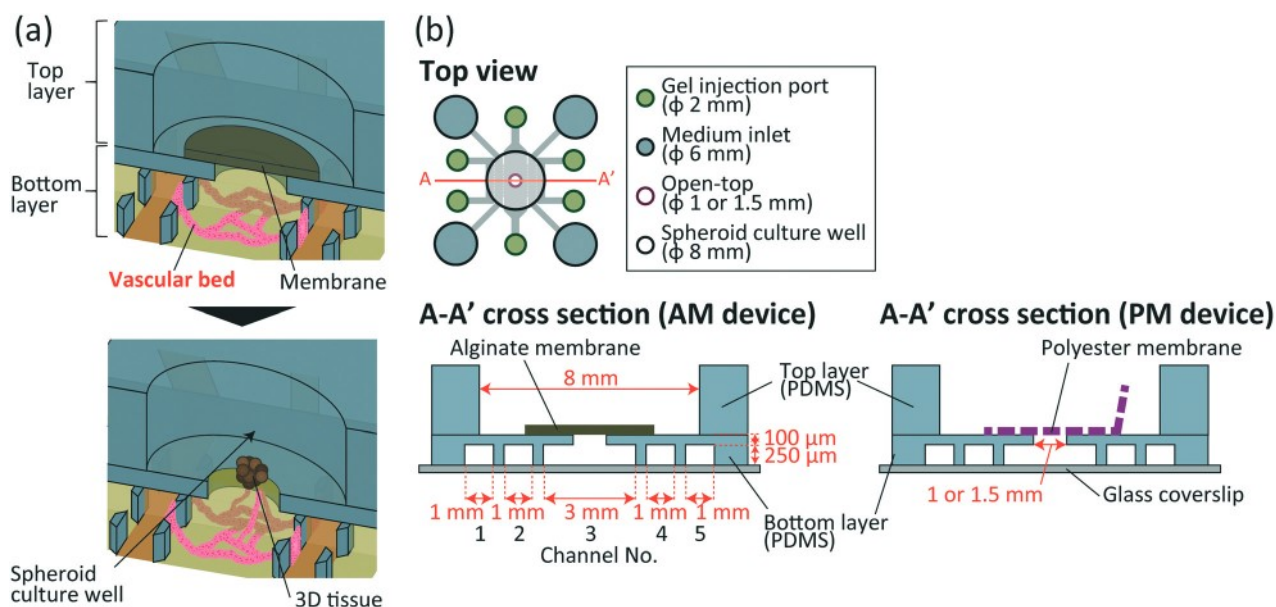


Fig. 1 Overview of the on-chip vascular bed method and the design of the microfluidic device. (a) The vascular bed is formed in the bottom layer. The spheroid culture well and channels in the bottom layer are separated by a membrane (left). A spheroid is cultured directly on the hydrogel after removing the membrane. Finally, the vasculature in the spheroid and the vascular bed connects (right). (b) Top view (top) and cross section (bottom) of the microfluidic device. The device has four parts shown in the bottom schematic: a top layer (blue) includes gel injection ports, reservoirs, and a spheroid culture well; a bottom layer (blue) has five parallel channels partitioned by micro-posts; an alginate membrane (dark green) or a polyester membrane (purple); and a glass coverslip (grey).

a thickness of 250 μm . The wafer was treated with trichloro-(1*H*,1*H*,2*H*-perfluorooctyl)-silane (Sigma-Aldrich, St Louis, MO, USA) for easy removal, followed by PDMS pre-polymer (PDMS base: curing agent = 10:1 [w/w]; Dow Corning Toray, Tokyo, Japan). After being degassed in a vacuum chamber for 1 h, the wafer was spin-coated (400 rpm, 60 s) and cured at 70 $^{\circ}\text{C}$ for over 1 h, resulting in a bottom layer with a thickness of ~ 400 μm (Fig. 2a(i and ii)). Conversely, the spheroid culture well for the top layer (diameter: 8 mm) was punched from a PDMS slab using a biopsy punch. The top and bottom PDMS layers were irreversibly bonded using atmospheric plasma (40 s, 50 W, flow rate: 50 sccm, Femto Science, Hwaseong, Korea; Fig. 2a(iii)) followed by curing at 70 $^{\circ}\text{C}$ for 1 h. After the device had been removed from the mould, the open top, gel injection ports, and medium inlets were punched from a PDMS slab using biopsy punches of 1 or 1.5, 2, and 6 mm in diameter, respectively (Fig. 2a(iv and v)).

The device was then bonded to a glass coverslip (24 \times 24 mm, Matsunami Glass, Osaka, Japan) after plasma treatment, as described above (Fig. 2a(vi)), and cured at 70 $^{\circ}\text{C}$ overnight.

In the AM device, a thin alginate membrane was prepared by cross-linking sodium alginate with calcium ions (Fig. 2b).²⁸ An alginate solution was prepared from 2% (w/v) sodium alginate (Kimica, Tokyo, Japan) in deionised water, while a cross-linking solution was prepared by dissolving calcium chloride (Fujifilm Wako, Osaka, Japan) in deionised water containing 30% (v/v) ethanol (Fujifilm Wako) to suppress membrane swelling. A total of 3 mL of the alginate solution was poured into a 35 mm Petri dish (Fig. 2b(i)) and dried in an oven at 35 $^{\circ}\text{C}$ for over 24 h to obtain a sodium alginate membrane (Fig. 2b(ii)), which was removed from the Petri dish and immersed in the cross-linking solution for 1 h (Fig. 2b(iii)). After being washed with deionised water, the cross-linked membrane was sandwiched between two glass plates, clamped with clips, and dried at 35 $^{\circ}\text{C}$ for over 48 h to produce a membrane of ~ 40 μm in thickness (Fig. 2b(iv)). Finally, the membrane was cut into a round shape using a biopsy punch with a 5 mm diameter (Sterile Dermal Biopsy Punch, Kai Industries, Tokyo, Japan), bonded to the open top of the device using a thin PDMS pre-polymer layer as glue, and cured at 70 $^{\circ}\text{C}$ for 30 min (Fig. 2b(v)). The fabricated devices were sterilised in a box containing ethanol for over 24 h and then dried at 70 $^{\circ}\text{C}$ for 1 h before use.

In the PM device, the membrane was prepared by cutting a polyester membrane with 0.4 μm diameter pores (Sterilitech, Kent, WA, USA). The membrane consisted of a circular body (diameter: 6 mm) and a rectangular tail (Fig. 2c(i)) that was bent for handling using tweezers (Fig. 2c(ii)). One day before cells were injected into the device, the membrane was immersed in 0.5% 2-methacryloyl-oxethylphosphorylcholine polymer (MPC, Nichiyu, Tokyo, Japan) diluted in 70% ethanol for at least 10 min (Fig. 2c(iii)) to prevent gel adhesion to the membrane. After being washed with deionised water and dried, the membrane was placed on the open top (Fig. 2c(iv)). The fabricated devices were sterilised by exposure to UV radiation overnight.

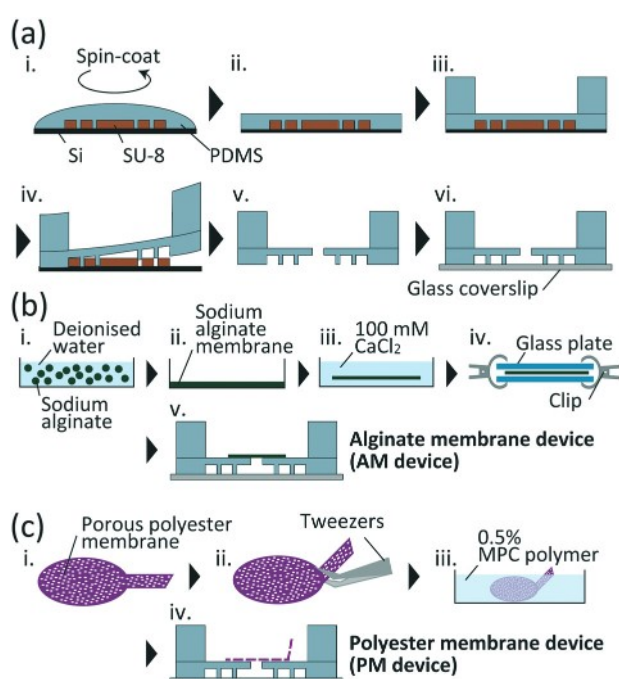


Fig. 2 Fabrication processes for the microfluidic device. (a) Fabrication of the device. i) PDMS pre-polymer was spin-coated onto the mould. ii) PDMS film (~ 400 μm) was used for the bottom layer. iii) The bottom and top layers were bonded. iv) The bonded layers were removed from the mould. v) An open top, gel injection ports, and medium inlets were punched out. vi) The device was bonded to a glass coverslip. (b) Alginate membrane preparation. i) Sodium alginate was dissolved in deionised water. ii) Sodium alginate solution was dried to produce a membrane. iii) The membrane was immersed in calcium solution containing ethanol to cross-link the sodium alginate with calcium ions. iv) The membrane was sandwiched between two glass plates to flatten it. v) The membrane was bonded to the open top using a thin PDMS pre-polymer layer as glue. (c) Polyester membrane preparation. i) A porous polyester membrane was cut out into the combined shapes of a circular body and a rectangular tail. ii) The rectangular tail was bent with tweezers. iii) One day before cell injection, the membrane was immersed in 0.5% MPC polymer for at least 3 min. iv) Finally, the membrane was settled on the device.

Optimisation of alginate membrane dissolution using EDTA

The concentration of EDTA and the exposure time of the alginate membrane to EDTA were optimised. Briefly, 5 μM FITC-dextran (70 kDa, Sigma) was added to the 2% (w/v) sodium alginate solution and used to fabricate an alginate membrane, as described in the 'Fabrication of the microfluidic device' section. The membrane was cut into a circle (diameter: 4 mm), placed into a 24-well plate (Corning, Corning, NY, USA), immersed in 500 μL of 0, 10, or 50 mM EDTA (Thermo Fisher Scientific, Waltham, MA, USA) diluted with phosphate-buffered saline (PBS), and incubated at 37 $^{\circ}\text{C}$. Membrane degradation was observed using a fluorescence microscope over 10 min. The average fluorescence intensity of the membrane was measured and

normalised to the initial fluorescence intensity for each condition.

Evaluation of non-adhesive polyester membrane with MPC coating

To confirm the efficacy of the MPC coating, we evaluated gel adhesion for non-coated and MPS-coated polyester membranes. A fibrin-collagen gel solution was prepared by mixing fibrinogen (5 mg mL⁻¹, Sigma), collagen type I (0.2 mg mL⁻¹, Corning), and aprotinin (0.15 U mL⁻¹, Sigma), as well as red fluorescent beads (0.2 μm diameter, Thermo Fisher Scientific; 1:100) to visualise adherence. After thrombin (0.5 U mL⁻¹ final concentration, Sigma) had been added to the solution, 30 μL was quickly injected into channel 3, and the gel was polymerised at 37 °C for 15 min. After the polyester membrane had been removed with tweezers, the adherence of the gel containing fluorescent beads was observed using a fluorescence microscope.

Cell culture

Unlabelled HUVECs (Angio Proteomie, Boston, MA, USA), green fluorescent protein-expressing HUVECs (GFP-HUVECs, Angio Proteomie), and red fluorescent protein-expressing HUVECs (RFP-HUVECs, Angio Proteomie) were cultured in endothelial cell growth medium-2 (EGM-2, Lonza, Basal, Switzerland), where the GA1000 supplied in the EGM-2 bullet kit was replaced with 1% penicillin and streptomycin (P/S, Thermo Fisher Scientific). Passage 4–6 cells were used for experiments. hLFs (Lonza) were cultured in fibroblast growth medium-2 (FGM-2, Lonza). Passage 4–5 cells were used for experiments. Mouse ASPS cells and red fluorescent protein (DsRed)-expressing ASPS cells were generated by introducing ASPSCR1-TFE3, a gene highly associated with ASPS, into embryonic mesenchymal cells.²⁵ The ASPS cells were cultured in Iscove's modified Dulbecco's medium with L-glutamine, HEPES, and sodium pyruvate (Fujifilm Wako) containing 10% fetal bovine serum (Thermo Fisher Scientific) and 1% P/S.

An hLF and HUVEC spheroid was prepared by mixing hLFs and RFP-HUVECs at a ratio of 4:1 (2.0 × 10⁴:5.0 × 10³ cells) in 200 μL of EGM-2. An ASPS spheroid was prepared by mixing hLFs, ASPS cells, and RFP-HUVECs, or hLFs, DsRed-ASPS cells, and HUVECs at a ratio of 2:2:1 (1.0 × 10⁴:1.0 × 10⁴:5.0 × 10³ cells) in 200 μL of EGM-2. The cell suspension was added into a 96-well plate with U-shaped bottom wells (Sumitomo Bakelite, Tokyo, Japan). The low-attachment surface of the wells reduced cellular adhesion and enabled spontaneous spheroid formation after 24 h incubation. The spheroid was transferred to the spheroid culture well in the microfluidic device. The total cell number (25 000 cells/spheroid) was adopted to obtain a spheroid with a diameter of 400 μm, in accordance with our previous study.^{16,17} The diameter was small enough to supply oxygen and nutrients to the inside of the spheroid as they are diffused up to 200 μm.²⁹

On-chip vascular bed formation

The cell seeding procedure is illustrated in Fig. S2.† Briefly, GFP-HUVECs (1.4 × 10⁷ cells mL⁻¹) and hLFs (1 × 10⁷ cells mL⁻¹) were suspended in EGM-2 and mixed at a ratio of 1:1 with a fibrin-collagen gel solution containing fibrinogen, collagen type I, and aprotinin at final concentrations in the cell suspension of 5 mg mL⁻¹, 0.2 mg mL⁻¹, and 0.15 U mL⁻¹, respectively. Thrombin (final concentration: 0.5 U mL⁻¹) was quickly added to the solution before 30 μL of HUVEC suspension (7 × 10⁶ cells mL⁻¹) was injected into channel 3, and 20 μL of hLF suspension (5 × 10⁶ cells mL⁻¹) was injected into channels 1 and 5. After gel polymerisation at 37 °C for 15 min, EGM-2 was introduced into the spheroid culture well and into channels 2 and 4. In the PM device, the polyester membrane was removed using tweezers, enabled by the non-adhesive MPC coating. The device was kept in a Petri dish covered with wet paper to prevent media evaporation.

After two days in culture, GFP-HUVECs (1 × 10⁵ cells in 20 μL EGM-2) were introduced into channel 2, and the device was incubated at 37 °C for 30 min at 90° to allow GFP-HUVECs to attach to the gel surface. This process was repeated in channel 4 to increase the possibility of opening the constructed vascular network into channels 2 and 4. The medium was changed every two days. On day 7, the vascular bed and spheroid co-culture was initiated. In the AM device, EGM-2 in the spheroid culture well was replaced with 50 mM EDTA, and the device was incubated at 37 °C for 10 min to dissolve the alginate membrane. The spheroid culture well was then washed three times with EGM-2 to remove alginate membrane debris and the remaining EDTA. In the PM device, the open top was already exposed to air after membrane removal. After EGM-2 had been removed from the spheroid culture well, a spheroid was transferred to the well and incubated at 37 °C for 1 h. Once the spheroid had settled on the gel, the spheroid culture well was filled with fresh EGM-2.

The perfusability of the vascular bed was examined on day 7 by introducing a fluorescent dye, 10 μM rhodamine-dextran (70 kDa, Sigma) in Dulbecco's phosphate-buffered saline (DPBS), into channel 4 after EGM-2 had been removed from all reservoirs. The solution was perfused by the pressure difference caused by the head difference between channels 2 and 4. After fluorescence images had been taken, the images were divided into four areas and fluorescence intensity was measured in the intra- and extravascular regions.

To evaluate the permeability of the vascular bed, the permeability coefficient of rhodamine-dextran across the bed was measured, and the coefficient P was calculated as follows:³⁰

$$P = \frac{1}{L_w} \times \frac{A}{I_{in}} \times \frac{dI_{ex}}{dt},$$

where L_w is the length of the vessel wall, A is the area of the extravascular region, I_{in} and I_{ex} are the mean fluorescence intensity in the intra- and extravascular regions, respectively,

and t is time. The intra- and extravascular regions and vessel wall length were measured from fluorescence images.

Evaluation of co-culture between spheroids and the vascular bed

The connection between the vascular bed (GFP-HUVECs) and spheroid vasculature (RFP-HUVECs) was confirmed by confocal microscopy as well as the fluorescence intensity profiles of RFP and GFP. The confocal image close to the boundary between the vascular bed and the spheroid was analysed. First, the image was smoothed using a Gaussian filter, and a line was defined across the vasculature. Next, RFP and GFP fluorescence intensities were measured along the line and normalised to their respective maximum intensities. The regions where both RFP and GFP intensity were less than a quarter of the maximum fluorescence intensity were defined as extravascular. The connection between the vascular bed and spheroid vasculature was confirmed by detecting high RFP and GFP signals in intravascular regions.

To determine whether the solution flowed into the spheroid *via* the vascular bed after connection, a fluorescent dye (0.1 mg mL^{-1} Alexa Fluor® 647-conjugated bovine serum albumin [Alexa647-BSA, Thermo Fisher Scientific] in DPBS) was injected into channel 4, as described in the ‘On-chip vascular bed formation’ section. For a detailed analysis, the cryosectioned samples were prepared. Initially, PDMS around the spheroid was cut out by a 2 mm diameter biopsy punch (Fig. S3a(i)†). The spheroid on the vascular bed with PDMS was removed with tweezers and placed upside down on the glass coverslip. Then, OCT compound (Sakura Finetech Japan Co., Tokyo, Japan) was dropped onto the spheroid and frozen (Fig. S3a(ii)†). After removal from the glass coverslip, PDMS was peeled off from the spheroid (Fig. S3a(iii)†). The spheroid was embedded in OCT compound again and frozen to prepare a cryoblock (Fig. S3a(iv)†). The block was sectioned using a cryostat (Thermo Fisher Scientific) at $10 \mu\text{m}$ thickness (Fig. S3a(v)†). The image obtained was analysed to measure the fluorescent dye distribution. An RFP fluorescence image was binarised to define the spheroid vasculature (Fig. S3b(i, ii)†) and converted to a distance map image. It defines the distance x from the wall to the nearest vasculature (Fig. S3b(iii)†). The interior of the spheroid vasculature as well as the wall of the vasculature is defined as $x = 0$. Then, the distance x and the intensity of Alexa Fluor® 647 in the spheroid region were plotted (Fig. S3b(iv)†).

To compare the distribution of Alexa647-BSA in the spheroid depending on the presence or absence of the vascular bed, we prepared a spheroid cultured on a gel without construction of the vascular bed. Initially, the fibrin-collagen gel solution was injected into channels 1, 3, and 5 in the PM device. After gel polymerisation at $37 \text{ }^\circ\text{C}$ for 15 min, the polyester membrane was removed, and the ASPS spheroid was transferred to the spheroid culture well and incubated at $37 \text{ }^\circ\text{C}$ for 1 h. Once the spheroid had settled on

the gel, the spheroid culture well and channel 4 were filled with EGM-2 and Alexa647-BSA, respectively. After Alexa647-BSA had fully diffused into the gel, the spheroid was observed and analysed following the procedure described above.

Imaging

Time-lapse bright field and fluorescence images were captured using an inverted microscope (CKX53, Olympus, Tokyo, Japan). Fluorescence images and cross-sectional images were acquired using a confocal microscope (FV3000, Olympus). The obtained images were analysed using ImageJ software (National Institutes of Health, Bethesda, MD, USA). Figure preparation and statistical analysis were performed by GraphPad Prism (GraphPad Software, San Diego, CA, USA) and MATLAB (MathWorks, Natick, MA, USA).

Results

Optimised EDTA concentration for dissolving the alginate membrane and non-adhesive MPC coating for the polyester membrane

First, we optimised the conditions for alginate membrane dissolution using EDTA in the AM device. Compared to the PBS-treated control, the fluorescence intensity of membranes in 10 and 50 mM EDTA decreased in a time-dependent manner (Fig. 3a). Although the membranes eventually

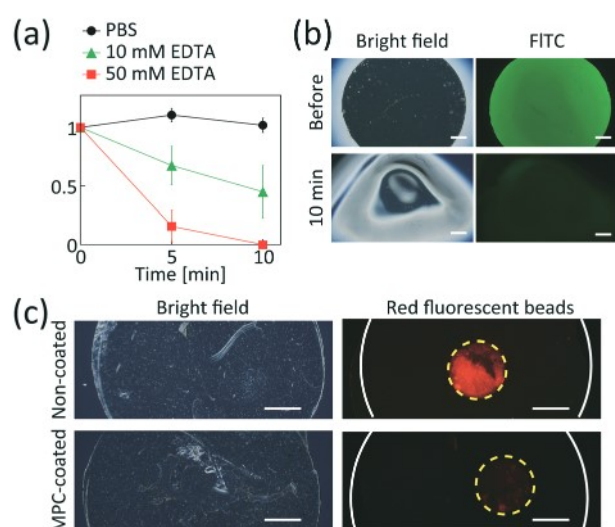


Fig. 3 Preparation of the alginate and polyester membranes. (a) Optimisation of EDTA concentration for dissolving the alginate membrane. Time-course of fluorescence intensity of the alginate membrane for three EDTA concentrations. The value was normalised to the initial intensity for each condition ($n = 3$). Error bars represent the S.E. (b) Bright field (left) and fluorescence (left) images of an alginate membrane including FITC-dextran before and 5 min after immersion in 50 mM EDTA. Green: FITC. Scale bars: $500 \mu\text{m}$. (c) Non-adhesive MPC coating for the polyester membrane. Bright field (left) and fluorescence images (right) of non-coated and MPC-coated membranes. White lines indicate the edge of the membrane. Yellow dotted lines indicate the area where the membrane was attached to the gel in the open top. Red: red fluorescent beads. Scale bars: 1 mm.

dissolved at both concentrations, 50 mM EDTA was required to completely dissolve the membrane within 10 min (Fig. 3b). We also tested alginate lyase, an alternative reagent for alginate membrane dissolution. It took 3 h to completely dissolve the membrane by 1 mg mL⁻¹ lyase, much longer than EDTA (Fig. S4†). Therefore, we used 50 mM EDTA diluted with PBS for 10 min in subsequent experiments.

In the PM device, we evaluated fibrin-collagen gel adhesion for non-coated and MPC-coated polyester membranes. When the membrane was uncoated, red fluorescent beads included in the gel were observed on the membrane, whereas almost no beads were detected on the MPC-coated membrane (Fig. 3c). Together, these findings confirm that the MPC coating prevents gel adhesion and facilitates the removal of the membrane after gel injection.

Formation of the perfusable vascular bed

After cells had been injected into channel 3, we confirmed that there was no gel leakage into channels 2 and 4 *via* the micro-posts on day 0 (Fig. 4a(i, ii, v and vi)). Moreover, both the alginate and polyester membranes blocked gel leakage from channel 3 into the spheroid culture well. On day 2, the HUVECs formed a vascular network in channel 3 due to the hLF secretions from channels 1 and 5 (Fig. 4a(iii and vii)). After one week, the vascular bed had been successfully

constructed in both devices (Fig. 4a(iv and viii)), and its lumen structures were observed (Fig. 4b and c).

Rhodamine-dextran solution was injected into channel 4 and flowed out into channel 2 through the vascular bed (Fig. 4d and Movie S1†). The fluorescence intensity in the intravascular region increased rapidly and reached levels approximately four times higher than that in the extravascular region (Fig. 4e), indicating that the fluorescent dye was retained inside the vascular bed. In addition, the fluorescence intensity in the extravascular region increased gradually due to diffusion through the vascular walls, suggesting that these structures were permeable to the dye (Fig. 4e and f). The permeability coefficient of the bed was 1.12×10^{-5} mm s⁻¹ for 70 kDa rhodamine-dextran, consistent with previously reported values.^{16,23} Therefore, we concluded that the perfusable vascular bed had been constructed successfully.

Co-culture of an hLF and HUVEC spheroid with the vascular bed

Four days after the spheroid had been placed on the vascular bed in the PM device, three types of vasculatures composed of GFP-HUVECs, RFP-HUVECs, or both HUVECs were clearly observed (Fig. 5a). Scanning channel 3 from bottom to top using confocal microscopy revealed that the vascular bed was

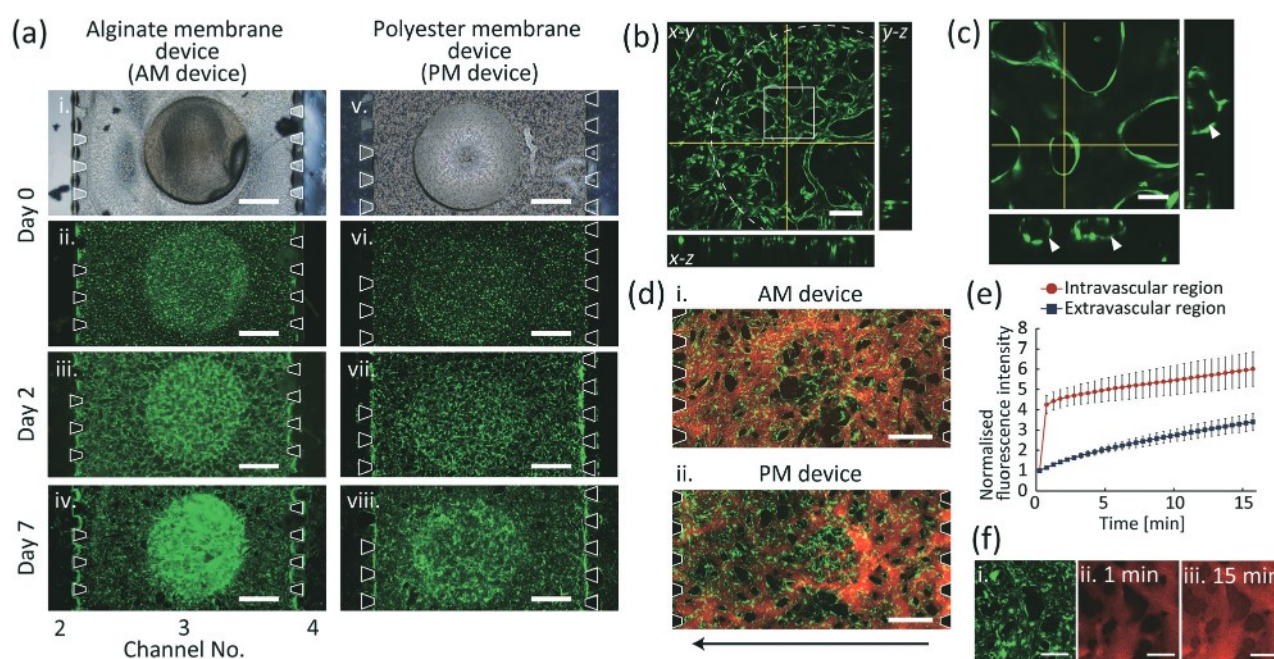
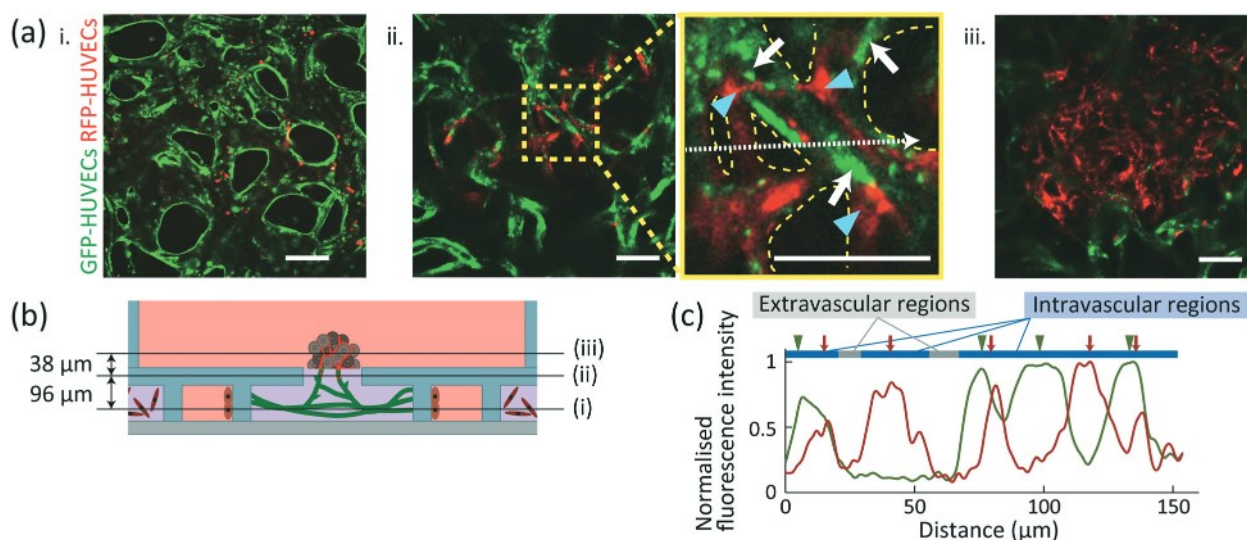


Fig. 4 Formation of the vascular bed in the microfluidic device. (a) Time lapse images of the construction of a vascular bed. (b) Orthogonal view from different planes (*x*-*y*, *x*-*z*, or *y*-*z*) of the confocal microscope. The vascular bed was formed in the PM device. The white dotted line indicates the edge of the open top. (c) Magnified view of the area indicated by the white rectangle in (b). White arrowheads indicate the vascular lumen. (d) Perfusion of the vascular bed. The black arrow indicates the direction of flow from channel 4 to channel 2. (e) Magnified view of the area indicated by the white rectangle in (d). (e) Time-course of fluorescence intensity in the intravascular and extravascular regions in (dii). The values were normalised to the initial intensity measured in each region and averaged ($n = 4$ areas in one device). Error bars represent the S.E. (f) Image of the vascular bed (i) and time-lapse images 1 min (ii) and 15 min (iii) after injection of rhodamine-dextran. Green: GFP-HUVECs, red: rhodamine-dextran. Scale bars: 500 μ m (a and d), 200 μ m (b and e), 50 μ m (c), 100 μ m (f).



Q4 Fig. 5 Co-culture of an hLF and HUVEC spheroid with a vascular bed in the PM device. (a) Confocal images of the bottom (i), middle (ii), and top (iii) levels. In the middle level, the vasculature, indicated by the yellow dashed line, was composed of GFP-HUVECs from the vascular bed (white arrows) and RFP-HUVECs from the spheroid (blue arrowheads). Green: GFP-HUVECs. Red: RFP-HUVECs. Scale bars: 100 μm. (b) Schematic cross-sectional diagram of the microfluidic device. The fluorescence images in (a) were captured at the levels indicated. (c) Intensity profile of RFP and GFP corresponding to the white dotted arrow scan in (a)(ii) right. Green arrowheads and red arrows indicate peaks of GFP and RFP fluorescence, respectively. Grey and blue bars indicate the extravascular and intravascular regions, respectively.

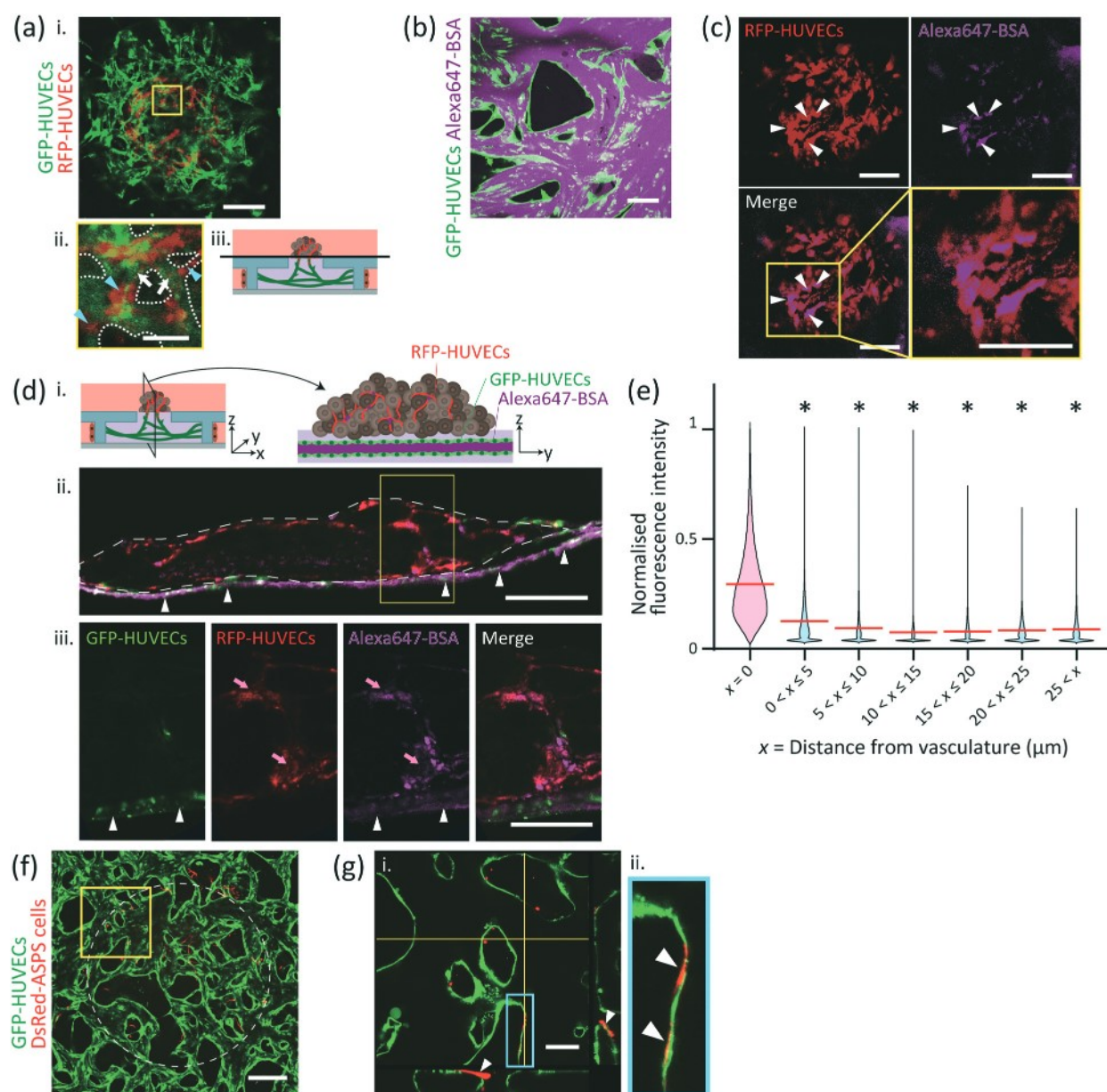
composed of GFP-HUVECs (Fig. 5a(i) and b(i)). Moreover, vasculature composed of both GFP-HUVECs and RFP-HUVECs was observed at the middle level, demonstrating a connection between the vascular bed and spheroid vasculature (Fig. 5a(ii) and b(ii)), whereas spheroid vasculature composed of only RFP-HUVECs was observed at the top level (Fig. 5a(iii) and b(iii)). The RFP and GFP fluorescence intensity profiles are shown in Fig. 5c along the line set to cross the vasculature in the right panel of Fig. 5a(ii). Extravascular regions were defined as those in which both RFP and GFP intensities were less than a quarter of the maximum fluorescence intensity (Fig. 5c, grey bars). All remaining regions were judged as intravascular regions and were found to display high RFP and GFP signals (- Fig. 5c, blue bars). Together, these findings suggest that the vasculature was composed of both GFP-HUVECs from the vascular bed and RFP-HUVECs from the spheroid, and that the vascular bed was successfully anastomosed to the spheroid. A similar connection was also observed in the AM device (Fig. S5†).

Co-culture of an ASPS spheroid with the vascular bed

Similar to the hLF and HUVEC spheroid, a connection between the vascular bed (GFP-HUVECs) and spheroid vasculature (RFP-HUVECs) was observed five days after the ASPS spheroid was placed on the vascular bed in the PM device (Fig. 6a). When injected into channel 4, the Alexa647-BSA dye solution flowed through the vascular bed (Fig. 6b), indicating that it retained perfusability during co-culture with the spheroid. Moreover, the fluorescent dye was detected inside the

spheroid vasculature composed of RFP-HUVECs (Fig. 6c). When the spheroid was sectioned, Alexa647-BSA was observed not only in the GFP-positive areas under the spheroid corresponding to the vascular bed (- Fig. 6d, white arrowheads), but also in the RFP-positive areas corresponding to the spheroid vasculature (- Fig. 6d, pink arrows). Fig. 6e shows the distribution of Alexa647-BSA intensity categorised according to the distance from the spheroid vasculature. In the spheroid vasculature ($x = 0 \mu\text{m}$), a wide range of fluorescence intensity was detected. The probability of the fluorescence intensity peaked at around 0.2. In contrast, most values of the normalised fluorescence intensity were clustered below 0.1 at the outside of the spheroid vasculature ($x > 0 \mu\text{m}$). The mean fluorescence intensity was significantly higher in the spheroid vasculature than that in the outside areas. This result indicated the presence of Alexa647-BSA in the spheroid vasculature. In contrast, when Alexa647-BSA was injected into the device where the spheroid was cultured on the gel without the vascular bed, after incubation for one day, the dye was not detected in the spheroid vasculature (Fig. S6†), suggesting that the dye did not flow into the spheroid vasculature merely by diffusion. Thus, we conclude that Alexa647-BSA detected in the spheroid vasculature in Fig. 6 flowed in *via* the vascular bed.

When DsRed-ASPS cells were used as spheroids, some cells migrated from the spheroid to the vascular bed region and attached to the vascular bed wall four days after spheroid injection (Fig. 6f and g). ASPS cell migration was also observed in the device integrated with a PDMS porous membrane (a similar design to that of a



Q6 Q5 Fig. 6 Co-culture of an ASPS spheroid with a vascular bed in the PM device. (a) Confocal images that focus on vascular connections. Magnified view of the area indicated by the yellow rectangle in (i) is shown in (ii). The fluorescence image was captured at the level indicated in (iii). The vasculature, indicated by the white dashed line, was composed of GFP-HUVECs from the vascular bed (white arrows) and RFP-HUVECs from the spheroid (blue arrowheads). (b) Fluorescence image of the vascular bed taken after Alexa647-BSA was injected. (c) After Alexa647-BSA injection, the dye was detected in vasculature composed of RFP-HUVECs in the spheroid (white arrowheads). (d) Confocal images of the cryosectioned spheroid. The spheroid was vertically sectioned as illustrated in (i). The dye was detected in the vascular bed (white arrowheads) and the spheroid vasculature (pink arrows). The spheroid region was indicated by the white dotted line. (e) Distribution of the Alexa647-BSA fluorescence intensities measured in different distances from vasculature. Red bars indicate the mean fluorescence intensities. $n = 50\,000$ – $200\,000$ pixels. $*p < 0.05$ vs. $x = 0\ \mu\text{m}$ group by Dunn's test. (f) Confocal image to detect the migration of ASPS cells. The white dotted line indicates the edge of the open top. (g) Magnified view of the area indicated by the yellow rectangle in (d). Magnified view of the area indicated by the blue rectangle in (i) is shown in (ii). Some migrating ASPS cells wrapped the vascular bed (white arrowheads). Green: GFP-HUVECs. Red: RFP-HUVECs (a, d and f), DsRed-ASPS cells (g and h). Magenta: Alexa647-BSA. Scale bars: $200\ \mu\text{m}$ (a(i) and g), $50\ \mu\text{m}$ (a(ii) and d(ii), h), $100\ \mu\text{m}$ (b–d(i)).

previous publication).²⁴ However, the number of ASPS cells that migrated was significantly more in our device (Fig. S7†), demonstrating that the direct contact between the spheroid and the vascular bed promoted their interaction, whereas a porous membrane between them limited the interaction.

Discussion

3D tissue culture is a powerful tool for understanding physiological events; however, a lack of nutrients and oxygen supply through vasculature currently limits the size, culture time, and maturity of 3D tissues. In this study, we proposed

1 a new method for culturing a tissue spheroid directly on an
2 'on-chip vascular bed'. The growth factors for vascular bed
3 formation secreted from hLFs were supplied from the side
4 channels (1 and 5), meaning that a perfusable vascular bed
5 was successfully constructed without relying on growth
6 factors from the 3D tissue.

7 In the AM device, an alginate membrane was used to
8 separate the spheroid culture well and the vascular area
9 (channel 3), by optimising the conditions for membrane
10 dissolution using EDTA. To prepare the alginate membrane,
11 we attempted cross-linking before drying the sodium alginate
12 solution (pre-drying process), as well as cross-linking after
13 drying the solution (post-drying process). Two processes have
14 an effect on alginate chain entanglement, which affects
15 polymer swelling by the absorption of water. First, in the
16 post-drying process, the sodium alginate solution was
17 initially gelled by cross-linking sodium alginate (1% and 4%
18 [w/v]) with calcium ions of a calcium chloride solution
19 carried by a cellulose membrane filter (Fig. S8a(i, ii)†). After
20 the gelation, the membrane was dried (Fig. S8a(iii, iv)†).
21 However, after a HUVEC suspension in fibrin-collagen gel
22 had been injected into the device, the membrane absorbed
23 water and became wrinkled due to swelling when 1% (w/v)
24 sodium alginate solution was used, causing the membrane to
25 adhere to the bottom glass coverslip, removing HUVECs from
26 the area (Fig. S8b†). Although this adhesion was overcome by
27 increasing the concentration of sodium alginate to 4% (w/v),
28 which increased alginate chain entanglement, the membrane
29 still became wrinkled (Fig. S8c†). These results indicate that
30 the post-drying process does not achieve sufficient alginate
31 chain entanglement to suppress swelling, with either the
32 sodium alginate solution of 1% or 4% (w/v), due to water
33 contained in the solution during cross-linking. Second, in
34 contrast to the post-drying process, the pre-drying process
35 resulted in much higher alginate chain entanglement by
36 causing the evaporation of water from the solution, reducing
37 water absorption and significantly reducing swelling of the
38 membrane.

39 Although the optimised alginate membrane enabled stable
40 vascular bed formation, the preparation of this device was
41 time-consuming as the thin and fragile membrane had to be
42 handled carefully. Therefore, we also attempted to use a
43 commercialised polyester membrane to seal the open top
44 during gel injection, which was subsequently removed after
45 gelation and 'on-chip vascular bed' construction, allowing for
46 direct contact between the spheroid and the vascular bed.
47 After several days in co-culture, we observed direct contact
48 between ECs from the spheroid and the 'on-chip vascular
49 bed', and confirmed that solution passed through the
50 vascular bed into the spheroid. Consequently, these findings
51 indicate that our method could be used to investigate the
52 effects of vasculature on 3D tissues. For example, mechano-
53 signalling pathways would be interesting targets as blood
54 flow is known to play important roles in the maturity and
55 morphology of 3D tissues *in vivo*. Indeed, modulating P2X4
(ref. 31) and VEGF signalling pathways by varying shear

56 stress³² could improve our understanding of mechano-
57 signalling pathways.

58 We demonstrated the applicability of our system using
59 ASPS spheroids. ASPS is a slow-growing but highly metastatic
60 sarcoma that is resistant to standard chemotherapy;
61 therefore, understanding the metastatic mechanisms of ASPS
62 could help in designing novel therapies. When the ASPS
63 spheroid was cultured on the vascular bed, we found that
64 some ASPS cells migrated and wrapped around the vascular
65 bed, but no other metastatic events, such as intravasation or
66 extravasation, were observed.

67 In metastasis, cancer cells initially migrate into the ECM
68 and attach to the vascular wall. After the cells have
69 intravasated, they are transported *via* blood and eventually
70 penetrate the vascular wall to form secondary cancers.
71 Therefore, intravasation and extravasation are essential to
72 metastasis. Recent studies have proposed a different
73 metastatic mechanism known as the 'invasion-independent
74 metastasis model', which does not require the invasion of
75 the vascular wall.³³ Firstly, cancer tissue induces
76 angiogenesis and acquires abundant vasculature, which
77 divides the cancer tissue into endothelium-coated small
78 clusters termed vessels encapsulating tumour clusters
79 (VETCs).³⁴ These VETCs are then shed into the blood and
80 migrate while maintaining cluster structures. It is thought
81 that ECs surrounding the VETCs protect cancer tissue from
82 immune attack, which may increase the levels of metastasis.
83 Importantly, the invasion-independent metastasis model is
84 relevant to ASPS metastasis as previous histological
85 observations have revealed that intravascular ASPS cells can
86 form VETC-like clusters.³⁵ Moreover, this model supports our
87 experimental finding that ASPS cells migrated along the
88 vascular wall without invading intravascular regions.

89 Collectively, our vascular bed system demonstrated a
90 connection between an ASPS spheroid and the vascular bed,
91 the first critical step of ASPS metastasis. Our system could
92 thus be useful for investigating the metastatic mechanism of
93 ASPS. Recent studies have also indicated that pericytes may
94 play important roles in metastasis; for instance, a mouse
95 model displayed vasculature in an ASPS tissue covered with
96 pericytes.²⁵ This is a structural characteristic of ASPS as
97 cancer vasculature often lacks pericytes, resulting in leakage
98 and insufficient oxygen supply.³⁶ In addition, the same study
99 observed that VETCs were covered with both ECs and
100 pericytes.²⁵ Our group and others have already succeeded in
101 forming a vascular network in the presence of pericytes.³⁷
102 Since these techniques could be applied to our vascular bed
103 system, we believe that the combination of our model and
104 that using pericytes will help to clarify the role of pericytes in
105 ASPS metastasis.

106 Conclusions

107 In conclusion, we developed a 3D tissue model co-cultured
108 on an 'on-chip vascular bed', whose formation was
109 independent of growth factors secreted from the 3D tissue.

In addition, the dissolvable membrane enabled direct contact between the 3D tissue and the bed, meaning that the assay system can be utilised to study the effects of vasculature on any 3D tissue, even those that do not secrete angiogenic factors.


Funding

This research was supported by AMED under Grant Number JP17be0304205 and JP20cm0106277. Microfabrication was supported by the Kyoto University Nano Technology Hub.

Conflicts of interest

The authors have no conflicts of interest to declare.

Acknowledgements

We thank our technical staff (Aki Kubo and Mayumi Moriwake) for helping with device fabrication and Editage  (www.editage.com) for English language editing.

References

- M. Vinci, S. Gowan, F. Boxall, L. Patterson, M. Zimmermann, W. Court, C. Lomas, M. Mendiola, D. Hardisson and S. A. Eccles, *BMC Biol.*, 2012, **10**, 29.
- D. D. R. Sebinger, M. Unbekandt, V. V. Ganeva, A. Ofenbauer, C. Werner and J. A. Davies, *PLoS One*, 2010, **5**, 1–10.
- T. Takebe, K. Sekine, M. Enomura, H. Koike, M. Kimura, T. Ogaeri, R. R. Zhang, Y. Ueno, Y. W. Zheng, N. Koike, S. Aoyama, Y. Adachi and H. Taniguchi, *Nature*, 2013, **499**, 481–484.
- M. A. Lancaster, M. Renner, C. A. Martin, D. Wenzel, L. S. Bicknell, M. E. Hurles, T. Homfray, J. M. Penninger, A. P. Jackson and J. A. Knoblich, *Nature*, 2013, **501**, 373–379.
- N. Eguchi, I. Sora and K. Muguruma, *Biochem. Biophys. Res. Commun.*, 2018, **498**, 729–735.
- M. Takasato, P. X. Er, H. S. Chiu, B. Maier, G. J. Baillie, C. Ferguson, R. G. Parton, E. J. Wolvetang, M. S. Roost, S. M. C. De Sousa Lopes and M. H. Little, *Nature*, 2015, **526**, 564–568.
- R. Morizane, A. Q. Lam, B. S. Freedman, S. Kishi, M. T. Valerius and J. V. Bonventre, *Nat. Biotechnol.*, 2015, **33**, 1193–1200.
- A. Taguchi, Y. Kaku, T. Ohmori, S. Sharmin, M. Ogawa, H. Sasaki and R. Nishinakamura, *Cell Stem Cell*, 2014, **14**, 53–67.
- H. Tsujimoto, T. Kasahara, S. Sueta, T. Araoka, S. Sakamoto, C. Okada, S. I. Mae, T. Nakajima, N. Okamoto, D. Taura, M. Nasu, T. Shimizu, M. Ryosaka, Z. Li, M. Sone, M. Ikeya, A. Watanabe and K. Osafune, *Cell Rep.*, 2020, **31**, 107476.
- K. A. Homan, N. Gupta, K. T. Kroll, D. B. Kolesky, M. Skylar-Scott, T. Miyoshi, D. Mau, M. T. Valerius, T. Ferrante, J. V. Bonventre, J. A. Lewis and R. Morizane, *Nat. Methods*, 2019, **16**, 255–262.
- C. W. van den Berg, L. Ritsma, M. C. Avramut, L. E. Wiersma, B. M. van den Berg, D. G. Leuning, E. Lievers, M. Koning, J. M. Vanslambrouck, A. J. Koster, S. E. Howden, M. Takasato, M. H. Little and T. J. Rabelink, *Stem Cell Rep.*, 2018, **10**, 751–765.
- S. Sharmin, A. Taguchi, Y. Kaku, Y. Yoshimura, T. Ohmori, T. Sakuma, M. Mukoyama, T. Yamamoto, H. Kurihara and R. Nishinakamura, *J. Am. Soc. Nephrol.*, 2016, **27**, 1778–1791.
- T. Takebe, M. Enomura, E. Yoshizawa, M. Kimura, H. Koike, Y. Ueno, T. Matsuzaki, T. Yamazaki, T. Toyohara, K. Osafune, H. Nakauchi, H. Y. Yoshikawa and H. Taniguchi, *Cell Stem Cell*, 2015, **16**, 556–565.
- D. Huh, B. D. Matthews, A. Mammoto, M. Montoya-Zavala, H. Y. Hsin and D. E. Ingber, *Science*, 2010, **328**, 1662–1669.
- S. Kim, H. Lee, M. Chung and N. L. Jeon, *Lab Chip*, 2013, **13**, 1489–1500.
- Y. Nashimoto, T. Hayashi, I. Kunita, A. Nakamasu, Y. S. Torisawa, M. Nakayama, H. Takigawa-Imamura, H. Kotera, K. Nishiyama, T. Miura and R. Yokokawa, *Integr. Biol.*, 2017, **9**, 506–518.
- Y. Nashimoto, Y. Teraoka, R. Banan Sadeghian, A. Nakamasu, Y. Arima, S. Hanada, H. Kotera, K. Nishiyama, T. Miura and R. Yokokawa, *J. Visualized Exp.*, 2018, **2018**, 1–12.
- E. Sano, C. Mori, Y. Nashimoto, R. Yokokawa, H. Kotera and Y. Torisawa, *Biomicrofluidics*, 2018, **12**, 042204.
- T. Osaki, V. Sivathanu and R. D. Kamm, *Sci. Rep.*, 2018, **8**, 1–13.
- Y. Nashimoto, R. Okada, S. Hanada, Y. Arima, K. Nishiyama, T. Miura and R. Yokokawa, *Biomaterials*, 2020, **229**, 119547.
- J. Kim, M. Chung, S. Kim, D. H. Jo, J. H. Kim and N. L. Jeon, *PLoS One*, 2015, **10**, 1–15.
- V. S. Shirure, Y. Bi, M. B. Curtis, A. Lezia, M. M. Goedegebuure, S. P. Goedegebuure, R. Aft, R. C. Fields and S. C. George, *Lab Chip*, 2018, **18**, 3687–3702.
- M. Campisi, Y. Shin, T. Osaki, C. Hajal, V. Chiono and R. D. Kamm, *Biomaterials*, 2018, **180**, 117–129.
- S. Oh, H. Ryu, D. Tahk, J. Ko, Y. Chung, H. K. Lee, T. R. Lee and N. L. Jeon, *Lab Chip*, 2017, **17**, 3405–3414.
- M. Tanaka, M. Homme, Y. Yamazaki, R. Shimizu, Y. Takazawa and T. Nakamura, *Cancer Res.*, 2017, **77**, 897–907.
- C. P. Huang, J. Lu, H. Seon, A. P. Lee, L. A. Flanagan, H. Y. Kim, A. J. Putnam and N. L. Jeon, *Lab Chip*, 2009, **9**, 1740–1748.
- J. Yan, F. Chen and B. G. Amsden, *Acta Biomater.*, 2016, **30**, 277–284.
- J. Li, J. He, Y. Huang, D. Li and X. Chen, *Carbohydr. Polym.*, 2015, **123**, 208–216.
- F. A. Auger, L. Gibot and D. Lacroix, *Annu. Rev. Biomed. Eng.*, 2013, **15**, 177–200.
- H. Lee, S. Kim, M. Chung, J. H. Kim and N. L. Jeon, *Microvasc. Res.*, 2014, **91**, 90–98.
- K. Yamamoto, T. Sokabe, T. Matsumoto, K. Yoshimura, M. Shibata, N. Ohura, T. Fukuda, T. Sato, K. Sekine, S. Kato, M. Isshiki, T. Fujita, M. Kobayashi, K. Kawamura, H. Masuda, A. Kamiya and J. Ando, *Nat. Med.*, 2006, **12**, 133–137.

- 1 32 N. G. dela Paz, T. E. Walshe, L. L. Leach, M. Saint-Geniez and P. A. D'Amore, *J. Cell Sci.*, 2012, **125**, 831–843.
- 5 33 T. Sugino, T. Kusakabe, N. Hoshi, T. Yamaguchi, T. Kawaguchi, S. Goodison, M. Sekimata, Y. Homma and T. Suzuki, *Am. J. Pathol.*, 2002, **160**, 1973–1980.
- 34 J. H. Fang, H. C. Zhou, C. Zhang, L. R. Shang, L. Zhang, J. Xu, L. Zheng, Y. Yuan, R. P. Guo, W. H. Jia, J. P. Yun, M. S. Chen, Y. Zhang and S. M. Zhuang, *Hepatology*, 2015, **62**, 452–465.
- 35 N. Setsu, A. Yoshida, F. Takahashi, H. Chuman and R. Kushima, *Hum. Pathol.*, 2014, **45**, 137–142.
- 5 36 S. Morikawa, P. Baluk, T. Kaidoh, A. Haskell, R. K. Jain and D. M. McDonald, *Am. J. Pathol.*, 2002, **160**, 985–1000.
- 37 K. Haase, M. R. Gillrie, C. Hajal and R. D. Kamm, *Adv. Sci.*, 2019, **6**, 1900878.

10

15

20

25

30

35

40

45

50

55

Supplementary Information (SI) to accompany

**Three-dimensional tissue model in direct contact with an on-chip
vascular bed enabled by removable membranes**

Yoshikazu Kameda, Surachada Chuaychob, Miwa Tanaka, Yang Liu, Ryu Okada,

Kazuya Fujimoto, Takuro Nakamura, and Ryuji Yokokawa*

*Ryuji Yokokawa

Department of Micro Engineering

Kyoto University

Kyoto Daigaku-Katsura, Nishikyo-ku

Kyoto 615-8540, Japan

Tel/Fax: +81-75-383-3680

Email: yokokawa.ryuji.8c@kyoto-u.ac.jp

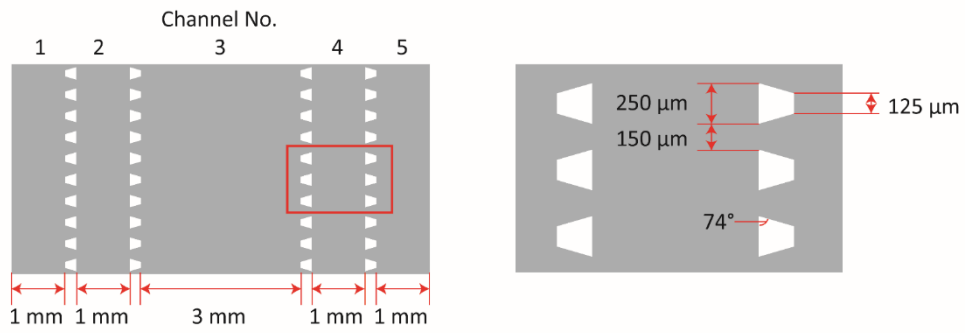


Fig. S1 Channel configuration. Dimensions for the micro-posts are shown in the enlarged illustration on the right. The grey area indicates fluid channels. The white trapeziums are micro-posts.

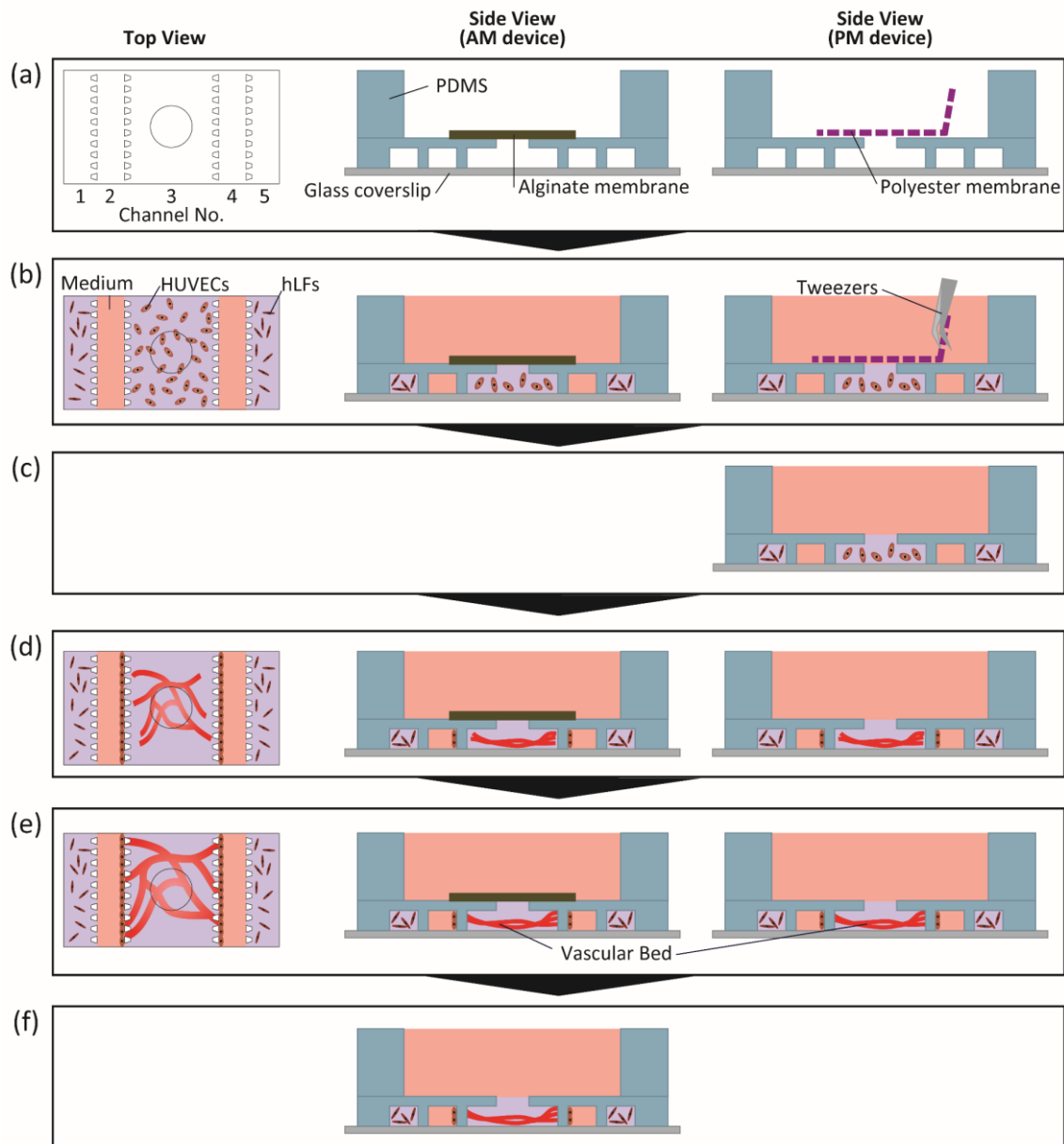


Fig. S2 Assay protocol for vascular bed formation. (a) The microfluidic device before seeding cells. (b) HUVECs were introduced into channel 3 and hLFs were introduced into channels 1 and 5. (c) In the PM device, the polyester membrane was removed using tweezers to open the open top after cell injection. (d) On day 2, HUVECs were introduced into channels 2 and 4. The device was tilted by 90° and incubated for 30 min, allowing HUVECs to adhere to the side of the gel in channel 3. (e) After one week in culture, the vascular bed was formed. (f) In the AM device, the alginate membrane was treated with EDTA to be dissolved before a spheroid was introduced.

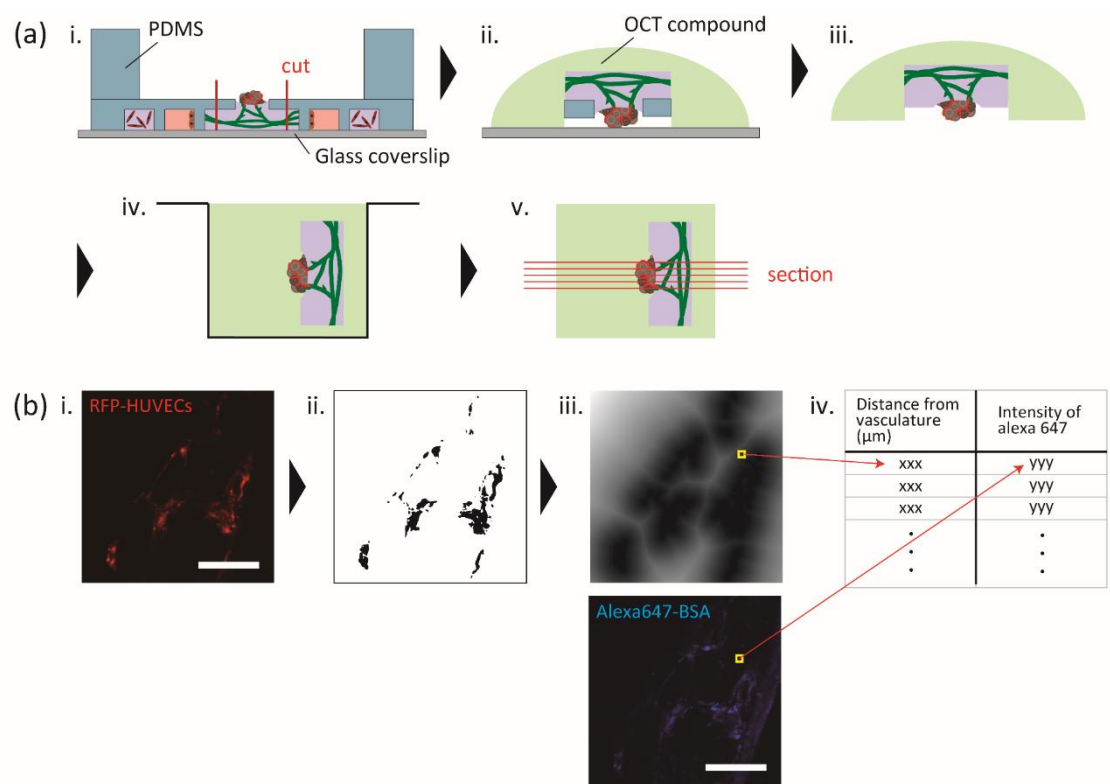


Fig. S3 Sample preparation and analysis procedure. (a) Preparation of the cryosectioned samples of the spheroid. i) PDMS around the spheroid was cut out with a biopsy punch (diameter: 2 mm). ii) The spheroid on the vascular bed with PDMS was removed using tweezers and placed upside down on the glass coverslip. Then, OCT compound was dropped onto the spheroid and frozen. iii) After removal from the glass coverslip, PDMS was peeled off from the spheroid. iv) The spheroid was embedded in OCT compound again and re-frozen to prepare a cryoblock. v) The block was sectioned using a cryostat. (b) Procedure to measure the fluorescent dye distribution. i) RFP fluorescence images were obtained. ii) The images were binarised. iii) The binarised images were converted to distance map images. iv) The distance x from the spheroid vasculature and the intensities of Alexa647-BSA in each pixel were measured using the distance map images and the fluorescence images, respectively. Scale bars: 50 μm .

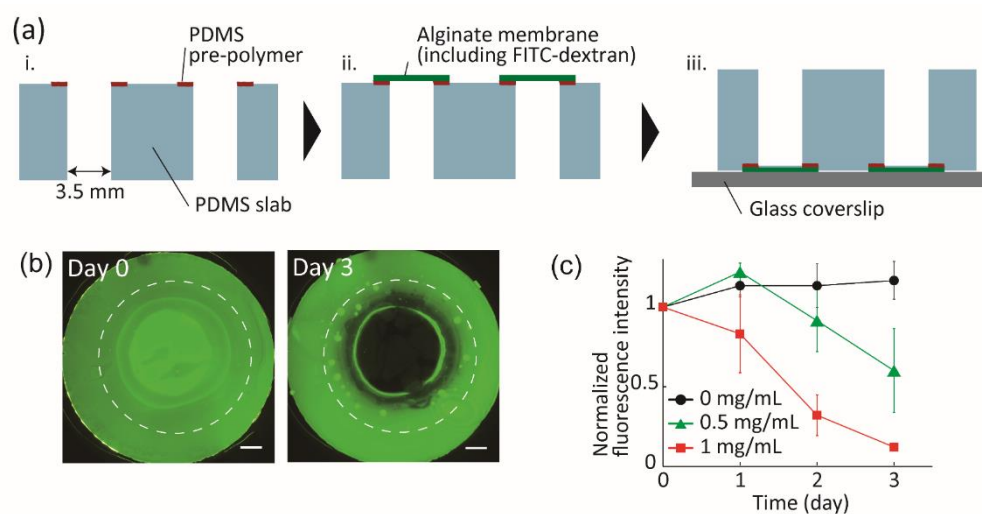


Fig. S4 Evaluation of alginate lyase for dissolving the alginate membrane. (a) Fabrication of wells for the alginate lyase evaluation. i) Wells (diameter: 3.5 mm) were punched out of a PDMS slab and PDMS pre-polymer was thinly coated around the wells. ii) Alginate membranes including FITC-dextran were bonded to the slab and cured at 70 °C for 30 min. iii) The PDMS slab was bonded to a glass coverslip using atmospheric plasma. The fabricated wells were filled with 30 μ L of EGM-2 containing alginate lyase (Alginate lyase S, Nagase ChemteX, Kyoto, Japan) at 0, 0.5, and 1 mg mL⁻¹, and incubated at 37 °C. Membrane degradation was observed under a fluorescence microscope over three days. The average fluorescence intensity in the well was measured and normalised to the initial fluorescence intensity for each condition. (b) Images of the alginate membrane including FITC-dextran before and three days after 1 mg mL⁻¹ alginate lyase was introduced. The white dashed circles indicate the area of the well. The fluorescence of FITC-dextran was no longer detected in the centre of the membrane within three days. Scale bars: 500 μ m. (c) Time-course of fluorescence intensity of the alginate membrane in three different concentrations of alginate lyase. It took three days to completely dissolve the membrane by 1 mg mL⁻¹ alginate lyase. Error bars represent the S.E.

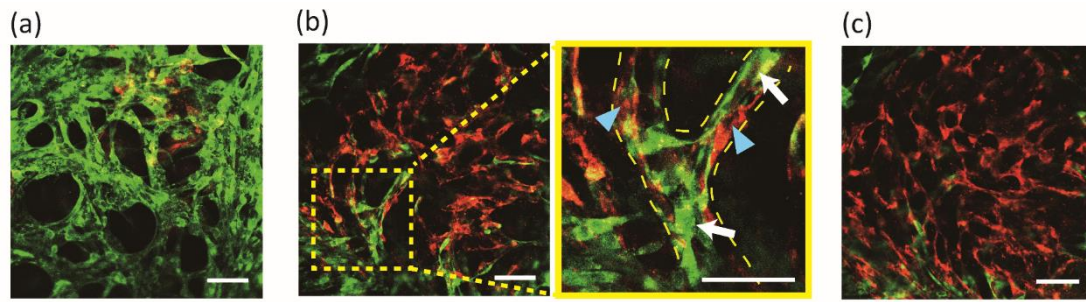


Fig. S5 Co-culture of an hLF and HUVEC spheroid with a vascular bed in the AM device. (a) Confocal images in the bottom (a), middle (b), and top (c) layers. In the middle layer, the vasculature, indicated by the yellow dashed line, was composed of GFP-HUVECs from the vascular bed (white arrows) and RFP-HUVECs from the spheroid (blue arrowheads). Green: GFP-HUVECs. Red: RFP-HUVECs. Scale bars: 100 μm .

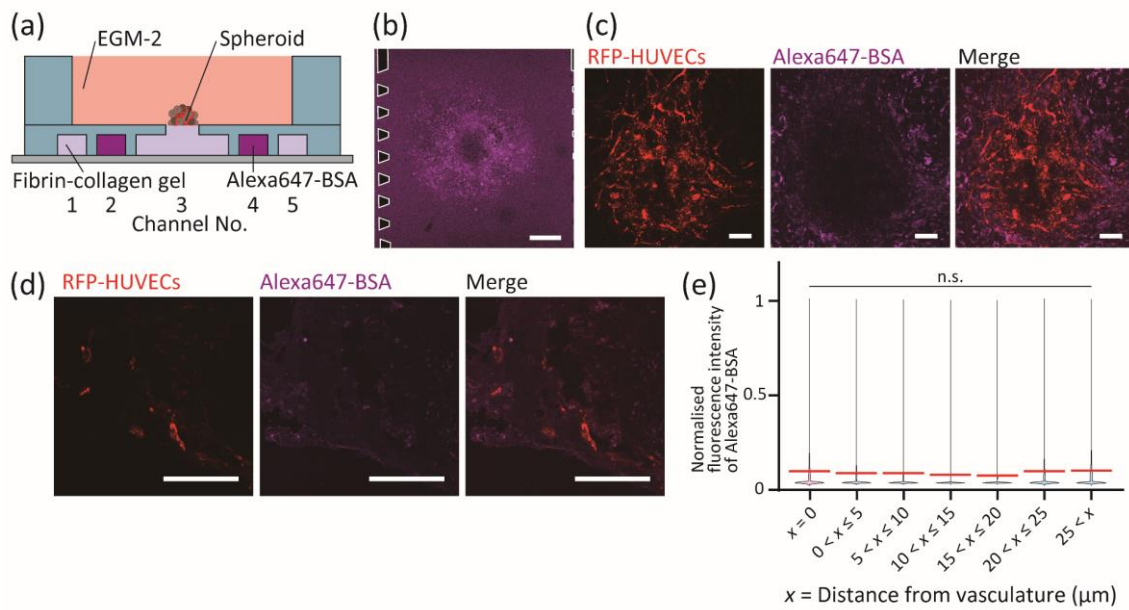


Fig. S6 Alexa647-BSA injection into the device where the spheroid was cultured on the gel. (a) Schematic diagram of the assay. (b) Confocal image in channel 3 one day after Alexa647-BSA injection. Alexa647-BSA fully diffused into the channel. (c) Confocal images of the spheroid. (d) Confocal images of the cryosectioned spheroid. (e) Distribution of the Alexa647-BSA fluorescence intensities categorised by distance from the vasculature. Red bars indicate the mean fluorescence intensities. The mean value and distribution of the fluorescence intensity were similar in the spheroid vasculature to the other areas. $n = 25,000\text{--}120,000$ pixels. $*p < 0.05$ vs. $0\ \mu\text{m}$ group by Dunn's test. Scale bars: $500\ \mu\text{m}$ (b), $100\ \mu\text{m}$ (c, d).

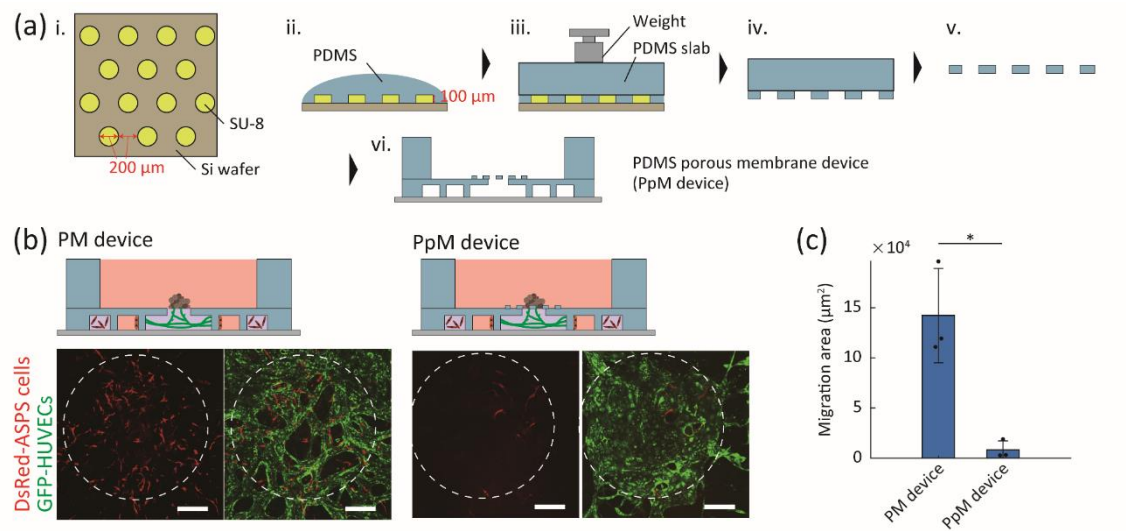


Fig. S7 Comparison of ASPS cell migration in the PM device and the device integrated with a PDMS porous membrane (PpM device). (a) Fabrication of the PpM device. i) The mould to fabricate the PDMS porous membrane. ii) Initially, PDMS pre-polymer was poured onto the mould. iii) The PDMS slab pre-treated with trichloro-silane was applied. Then, a 60 g weight was placed on the PDMS slab to allow SU-8 pillars to penetrate the uncured PDMS layer. iv) After curing at 70 °C overnight, the PDMS porous membrane was peeled off from the mould with the PDMS slab. v) The membrane was carefully peeled off from the PDMS slab. vi) Finally, the membrane was cut into a round shape using a biopsy punch with a 3 mm diameter and irreversibly bonded to the open top of the device using atmospheric plasma. (b) Confocal images taken after four days of co-culture with the ASPS spheroid and the vascular bed in the PM and PpM devices. The white dotted line indicates the edge of the open top. Scale bars: 200 μm. (c) Quantification of ASPS cell migration in the PM and PpM devices. After DsRed fluorescence images were binarised, DsRed positive areas were measured. Error bars represent the S.E. ($n = 3$ devices). * $p < 0.05$ by t -test.

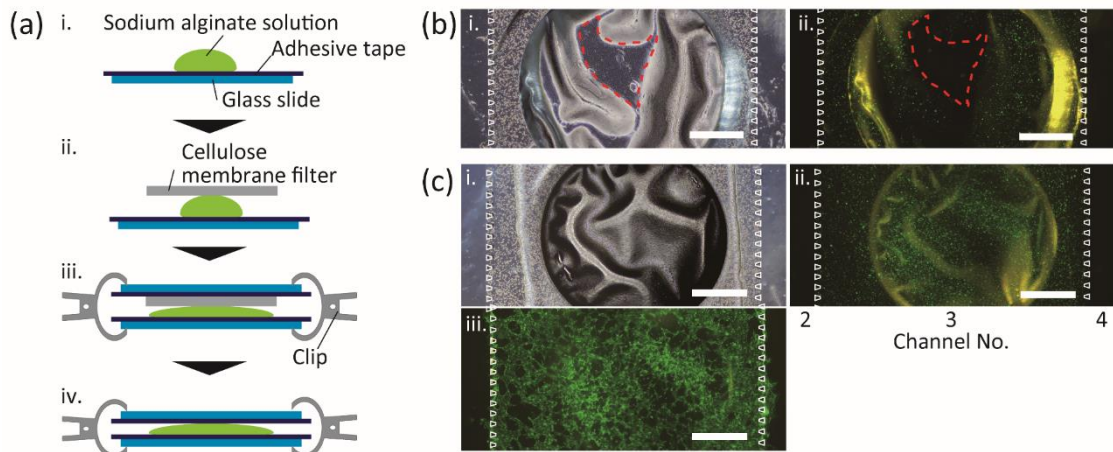


Fig. S8 Optimisation of the fabrication process of the alginate membrane. (a) Alginate membrane preparation. i) An alginate solution containing 1% or 4% (w/v) sodium alginate in deionised water was prepared. Then, 100 μ L of the solution was placed on a glass slide covered with adhesive tape. ii) A cellulose membrane filter (ADVANTEC, Tokyo, Japan) was immersed in 100 mM calcium chloride in deionised water for more than 1 min. The sodium alginate was cross-linked with calcium ions by placing the membrane filter on the sodium alginate solution for 1 min. iii) The other glass slide covered with adhesive tape was placed on the filter and clamped with clips for 10 min. The alginate gel was then thinned and flattened. iv) The cellulose membrane filter was removed, and the membrane was again sandwiched between two glass slides and dried at 70 $^{\circ}$ C for more than 1 day. Finally, the membrane was cut into a rectangular shape (ca. 4.5 \times 5 mm) to be bonded to the top PDMS layer. (b) Bright field (i) and fluorescence images (ii) after the injection of HUVECs into channel 3 with the 1% sodium alginate membrane. The membrane was attached to the bottom glass coverslip (the area indicated by the red dotted line) and HUVECs were removed from the area. (c) Bright field (i) and fluorescence images (ii) after the injection of HUVECs into channel 3 with a 4% sodium alginate membrane. (iii) A fluorescence image on day 6 after HUVEC injection. Green: GFP-HUVECs. Scale bars: 1 mm (b, c).

Movie S1

Flow of rhodamine-dextran (70 kDa) from channel 4 to channel 2 through the vascular bed in the PM device (x20 speed). Green: GFP-HUVECs, Red: Rhodamine-dextran.